

Network Coding in Cooperative Communications: Friend or Foe?

Sushant Sharma, *Member, IEEE*, Yi Shi, *Member, IEEE*,
Jia Liu, *Member, IEEE*, Y. Thomas Hou, *Senior Member, IEEE*,
Sastry Kompella, *Member, IEEE*, and Scott F. Midkiff, *Senior Member, IEEE*

Abstract—A major benefit of employing network coding (NC) in cooperative communications (CCs) is its ability to reduce time-slot overhead. Such approach is called network-coded CC (or NC-CC). Most of the existing works have mainly focused on exploiting this benefit without considering its potential adverse effect. In this paper, we show that NC may not always benefit CC. We substantiate this important finding with two important scenarios: employing analog network coding (ANC) in amplify-and-forward (AF) CC, and digital network coding (DNC) in decode-and-forward (DF) CC. For both scenarios, we introduce the important concept of *network coding noise* (NC noise). We analyze the origin of this noise via a careful study of signal aggregation at a relay node and signal extraction at a destination node. We derive a closed-form expression for NC noise at each destination node and show that the existence of NC noise could diminish the advantage of NC in CC. Our results shed new light on how to use NC in CC most effectively.

Index Terms—Cooperative communications, network coding, network coding noise.

1 INTRODUCTION

SPATIAL diversity, in the form of employing multiple antennas (i.e., MIMO), has shown to be very effective in increasing network capacity. However, equipping a wireless node with multiple antennas may not always be practical, as the footprint of multiple antennas may not fit on a wireless node (e.g., a handheld wireless device). In order to achieve spatial diversity without requiring multiple antennas on the same node, the so-called *cooperative communications* (CCs) could be employed [15], [16], [21]. Under CC, each node is equipped with only a *single* antenna and spatial diversity is achieved by exploiting the antennas on other (cooperative) nodes in the network.

A simple form of CC can be best illustrated by a three-node example shown in Fig. 1 [16]. In this figure, node s transmits to node d via one-hop, and node r acts as a cooperative relay node. Cooperative transmission from s to d is done on a frame-by-frame basis. Within a frame, there are two time slots. In the first time slot, source node s makes a transmission to destination node d . Due to the broadcast nature of wireless medium, transmission by node s is also overheard by relay node r . In the second time slot, node r

forwards the data it overhears in the first time slot to node d . At destination node d , the two copies of the data are combined and may improve the data rate between s and d .

This three-node example shows CC for a single source-destination session. In general, for multiple sessions sharing the same relay node, it will be necessary to divide a time frame into multiple mini-slots. For example, suppose there are N source nodes, N destination nodes, and one relay node. For the N source-destination pairs to take advantage of CC, one can divide a time frame into $2N$ mini-slots (see Fig. 2), with every two mini-slots assigned to a session. Note that among the $2N$ mini-slots, only N mini-slots are used for transmissions between source and destination nodes. The other N mini-slots are solely used for transmissions between the relay and destination nodes to complete CC for each of the N sessions. Obviously, this scheme is wasteful in terms of time slot usage.

A natural question to ask is the following: Is it possible to retain the benefits of CC while reducing its undesirable overhead (in terms of the required number of mini-slots for data relaying)? If this is possible, then the benefits of CC can be extended in a multisession communication environment.

It turns out that recent advances in *network coding* (NC) [1], [2], [17], [24], [25] offers a key to answer this question. Fig. 3 shows a time slot structure of CC with NC. Under this scheme, the source node of each session first transmits in its respective time slot. For a given source node, its transmission is received by the corresponding destination node, and overheard by the cooperative relay node and other destination nodes (see Figs. 4a, 4b, and 4c). After each source node takes turns to complete its transmission, the relay node performs a linear combination of all the signals that it has overheard in the previous N time slots. Then, the relay node broadcasts the combined signal to all the destination nodes in a *single* time-slot [the $(N + 1)$ th time slot in Figs. 3 and 4d]. Then, each destination node extracts

• S. Sharma is with the Computational Science Center, Brookhaven National Laboratory, Room 255, Building 463B, Upton, NY 11973. E-mail: sushant@bnl.gov.

• Y. Shi, Y.T. Hou, and S.F. Midkiff are with the Bradley Department of Electrical and Computer Engineering, Virginia Tech, Blacksburg, VA 24061. E-mail: {yshi, thou, midkiff}@vt.edu.

• J. Liu is with the Department of Electrical and Computer Engineering, Ohio State University, Room 364, Dreese Labs, 2015 Neil Avenue, Columbus, OH 43210. E-mail: liu@ece.osu.edu.

• S. Kompella is with the Information Technology Division, US Naval Research Laboratory, 4555 Overlook Avenue, SW, Washington, DC 20375. E-mail: sastry.kompella@nrl.navy.mil.

Manuscript received 27 May 2010; revised 19 Jan. 2011 and 16 May 2011; accepted 20 May 2011; published online 8 June 2011.

For information on obtaining reprints of this article, please send e-mail to: tmc@computer.org, and reference IEEECS Log Number TMC-2010-05-0255. Digital Object Identifier no. 10.1109/TMC.2011.130.

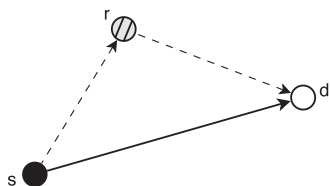
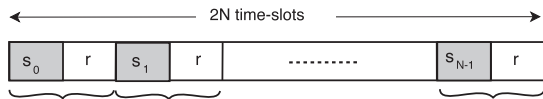


Fig. 1. A three-node schematic for CC.

Fig. 2. A frame structure for CC when there are N source-destination pairs sharing one relay node.

its desired signal by subtracting the overheard signals from the aggregated signal. We call this approach *network-coded CC* (or NC-CC). In the context of N source-destination example discussed, NC-CC offers a reduction of $(N - 1)$ time-slots compared to CC! Further, due to the reduction of the total number of time-slots in a frame, the duration of each time-slot (for transmission) is increased.

Ideally, after the relay node transmits the combined signal, we wish to extract the desired signal at each destination node as cleanly as possible. But as we shall show in Section 3, a perfect extraction is usually not possible. Just as one would expect, there is no “free lunch” here. In the context of analog network coding (ANC), Section 3.1 shows that there will be a nonnegligible noise introduced in the process. Similar situation also occurs in the context of digital network coding (DNC), which we will show in Section 3.2. We call such noise as “network coding noise” (or NC noise), which we find is the main “foe” in NC-CC.

Due to this foe, we find that employing NC in CC may not always be advantageous. To substantiate this finding, we perform an in-depth analysis of NC-CC in the context of 1) ANC [12], [19] with amplify-and-forward (AF) CC [16] (denoted as ANC-CC), and 2) DNC [11] with decode-and-forward (DF) CC [16] (denoted as DNC-CC). The main results of this paper are as follows:

- We formalize the important concept of NC noise, which we find is the main foe in NC-CC.
- We derive closed form expressions for ANC and DNC noise by studying the signal aggregation process at a relay node and the signal extraction process at a destination node. We also derive mutual information and achievable rate under ANC-CC and DNC-CC.
- Through extensive numerical results, we show the impact of NC noise on NC-CC. Our results offer a new understanding on how to use NC in CC most effectively in light of NC noise.

The remainder of this paper is organized as follows. Section 2 presents related work. In Section 3, we offer an overview of the problems associated with NC-CC in the context of ANC and DNC. In Section 4, we consider ANC-CC and offer a theoretical analysis for the origin of NC noise. We give a mathematical characterization of ANC noise and show how to compute mutual information and achievable rate for each session. In Section 5, we perform a

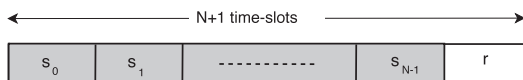
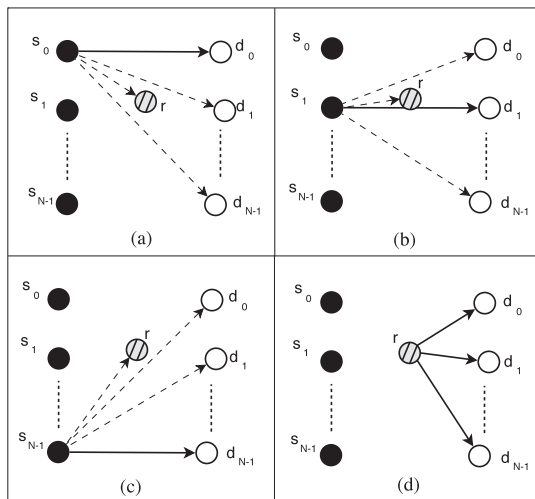


Fig. 3. Time slot structure for CC with NC.

Fig. 4. Sequence of transmissions at N source nodes and the single relay node.

parallel study for DNC-CC. Section 6 presents numerical results and shows the impact of NC noise on NC-CC. Section 7 concludes this paper.

2 RELATED WORK

In this section, we briefly review related work in CC and NC. We also review several recent efforts on NC-CC.

The concept of CC can be traced back to the three-terminal communication channel (or a relay channel) in [23] by Van Der Meulen. Shortly after, Cover and El Gamal studied the general relay channel and established an achievable lower bound for data transmission [4]. These two seminal works laid the foundation for the present-day research on CC. Recent research on CC aims to exploit distributed antennas on neighboring nodes in the network, and has resulted in a number of protocols at the physical layer [5], [6], [7], [9], [16], [18], [21], [22] and the network layer [13], [20], [27]. The AF CC and DF CC models used in our study in this paper are based on [16].

The concept of NC was first introduced by Ahlswede et al. in their seminal work [1], where they showed how NC can save bandwidth for multicast flows in a wired network. In the context of wireless networks, the most widely studied types of NC are DNC (see, e.g., [11]) and ANC (see, e.g., [12]). For the state of the art in NC, we refer readers to the NC bibliography in [8].

Recent efforts on NC-CC that are most relevant to our work include [2], [17], [24], [25]. Bao and Li [2] were the first to employ NC in CC in a multisource single-destination network. They showed that NC-CC can improve the achievable rate and outage probability of a network. Shortly after, Peng et al. [17] considered a network with a single relay node and multiple source-destination pairs. They again showed that NC can help CC reduce the outage probability of the entire network. More recently, Xiao et al. [24] considered a two-source single-destination network and showed that NC can help CC reduce packet error rates.

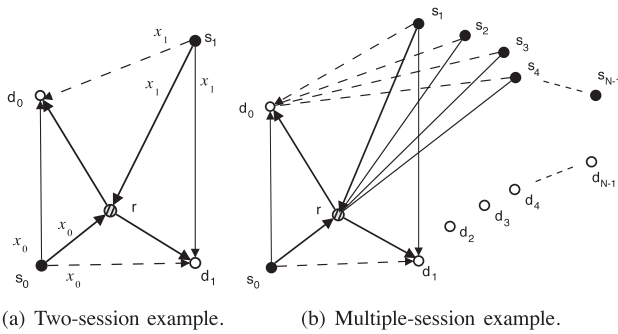


Fig. 5. Examples illustrating NC in CC.

In [25], Xu and Li considered a cellular network with bidirectional traffic, and showed that the network throughput can be increased when NC is employed in CC. These results all show the benefits of applying NC to CC. However, the potential “foe” in NC-CC has not been recognized and explored.

3 THE PROBLEM

In this section, we explore the potential foe in NC-CC in terms of NC noise. To start, we consider an example shown in Fig. 5a, where there are two source-destination pairs ($s_0 - d_0$ and $s_1 - d_1$) and one-relay node (r). Both source-destination pairs will use the same relay node for CC and NC is employed at the relay node.

3.1 Analog NC-CC

Based on our discussion for Fig. 3, a frame is divided into three time-slots. In the first time-slot, s_0 broadcasts signal x_0 to d_0 , which is overheard by r and d_1 ; in the second time slot, s_1 broadcasts signal x_1 to d_1 , which is overheard by r and d_0 ; then the relay node r performs ANC by combining the overheard signals from s_0 and s_1 , and then amplifies and broadcasts the combined signal in the third time slot to d_0 and d_1 . The destination node d_0 receives one copy of signal x_0 in the first time slot. It also overhears a copy of signal x_1 (denoted as $y_{s_1 d_0}$) in the second time slot. In the third time slot, destination node d_0 receives the combined signal, denoted as $y_{s_0 r d_0} + y_{s_1 r d_0}$.

One would hope that the destination node d_0 in Fig. 5a can cleanly extract $y_{s_0 r d_0}$ by having the combined signal ($y_{s_0 r d_0} + y_{s_1 r d_0}$) subtract the overheard signal $y_{s_1 d_0}$. But in reality, $y_{s_1 r d_0} \neq y_{s_1 d_0}$ due to two different paths. As a result of such subtraction, a new noise term, called “ANC noise” (for the analog version), will be introduced at d_0 . This noise term is $[y_{s_1 r d_0} - y_{s_1 d_0}]$. When the number of sessions increases (see Fig. 5b), the sum of noise will increase, and the aggregate noise at d_0 in Fig. 5b becomes $\sum_{i=1}^{N-1} [y_{s_i r d_0} - y_{s_i d_0}]$. That is, the amount of ANC noise grows as N increases. Clearly, the benefits of employing ANC will be diminished as ANC noise increases. For a given session, the mutual information (or achievable rate) is a good measure of the benefits of ANC-CC. We will show that the effective mutual information will decrease due to ANC noise.

3.2 Digital NC-CC

In the digital version, the signal combining procedure changes slightly at the relay node when it employs DNC

for DF CC. For the two-session example in Fig. 5a, source node s_0 transmits a signal in the first time slot. This signal is received and *decoded* by the relay node and overheard by the other destination node d_1 . Similarly, in the second time slot, source node s_1 transmits and the signal is received and decoded by r ; and overheard by d_0 . In the third time slot, the relay node combines the two decoded signals using DNC, and then transmits the combined signal. To extract the signal, the destination node d_0 subtracts the overheard signal (from s_1 in the second time slot) from the combined signal to obtain the desired signal. Again, due to different paths taken by the signals, the subtraction will result in a noise term, which we call DNC noise. It is easy to see that as the number of sessions on the relay node increase (as in Fig. 5b), the DNC noise will also increase. Similar to ANC-CC, the benefits of employing DNC will diminish as DNC noise increases, and so will the effective mutual information.

In the following two sections, we quantify the above discussion through a careful analysis of NC noise, both for analog and digital cases.

4 THE CASE OF ANC-CC

In this section, we focus on analog version of NC-CC. In Section 4.1, we analyze the ANC noise for ANC-CC. Then, in Section 4.2, we derive the achievable rate under ANC-CC in light of ANC noise. Table 1 shows all notation in this paper.

4.1 Analysis of ANC Noise

We first consider the simple two-session example in Fig. 5a. For this simple network, we analyze the ANC process at the relay node. Then, we analyze the signal extraction process of a destination node. This is followed by the derivation of ANC noise. Based on the results for the two-session case, we generalize the results for the N -session case shown in Fig. 5b.

4.1.1 Two-Session Case

In Fig. 5a, we assume that the signal x_0 transmitted by source s_0 in the first time slot is for packet p_0 , and the signal x_1 transmitted by source s_1 in the second time slot is for packet p_1 . We use $h_{s_0 d_0}$ to capture the effect of path-loss, shadowing, and fading between nodes s_0 and d_0 . Assume that the background noise at a node r , denoted by z_{rr} is white Gaussian with zero mean and variance σ_r^2 . Denote y_{srd} as the signal received by a destination node d that is transmitted by a relay node r and originated from some source s . Denote y_{sr} as the signal received by the relay node r that is transmitted and originated at some source s . Denote α_r as the amplifying factor used by the relay node r .

Combining signals at relay node. Since node s_0 transmits in the first time slot, we can express the signals received by r , d_0 , and d_1 during the first time slot as

$$y_{s_0 r} = h_{s_0 r} x_0 + z_r, \quad (1)$$

$$y_{s_0 d_0} = h_{s_0 d_0} x_0 + z_{d_0},$$

$$y_{s_0 d_1} = h_{s_0 d_1} x_0 + z_{d_1}. \quad (2)$$

TABLE 1
Notation

Symbol	Definition
$C_{\text{ANC-CC}}(s_i, r_j, d_i)$	Achievable rate for s_i - d_i pair with relay r_j under ANC-CC
$C_{\text{DNC-CC}}^{\text{UB}}(s_i, r_j, d_i)$	Upper bound on the achievable rate for s_i - d_i pair with relay r_j under DNC-CC
$C_{\text{DNC-CC}}^{\text{LB}}(s_i, r_j, d_i)$	Lower bound on the achievable rate for s_i - d_i pair with relay r_j under DNC-CC
$C_{\text{AF}}(s_i, r_j, d_i)$	Achievable rate for s_i - d_i pair with relay r_j under AF CC (no NC)
$C_{\text{DF}}(s_i, r_j, d_i)$	Achievable rate for s_i - d_i pair with relay r_j under DF CC (no NC)
$C_{\text{D}}(s_i, d_i)$	Achievable rate for s_i - d_i pair under direct transmission
h_{uv}	Variable to capture the effect of path loss, shadowing and fading between nodes u and v
N	Number of source nodes in the network
r	Relay node
x_s	Signal transmitted by node s
y_{uv}	Received signal at node v (from node u)
$y_{(s_i \cup s_j)rd}$	Combination of analog signals from s_i and s_j received by destination node d (with NC at relay node r)
z_v	Background noise at node v
z_v^{ANC}	ANC noise at node v
z_v^{DNC}	DNC noise at node v
s_i	The i -th source node
S_r	Set of source nodes using relay node r to perform ANC-CC
SNR_{uv}	The signal noise ratio at node v when u is transmitting
W	Total bandwidth available in the network
P_u	Transmission power at node u
σ_v^2	Variance of background noise at node v
$\sigma_v^{\text{ANC}2}$	Variance of ANC noise at node v
$\sigma_v^{\text{DNC}2}$	Variance of DNC noise at node v
α_r	Amplifying factor at relay r for ANC-CC

In the second time slot, when node s_1 transmits, the signals received by r, d_0 , and d_1 can be expressed as

$$y_{s_1 r} = h_{s_1 r} x_1 + z_r, \quad (3)$$

$$y_{s_1 d_0} = h_{s_1 d_0} x_1 + z_{d_0},$$

$$y_{s_1 d_1} = h_{s_1 d_1} x_1 + z_{d_1}.$$

Then, in the third time slot, relay node r combines x_0 and x_1 , and amplifies and broadcasts the combined signal. Fig. 6 shows the transmission behavior of ANC-CC for two sessions.

Signal extraction at a destination node. To understand how a destination node will separate this combined signal, we focus on one of the destination nodes, d_1 . At d_1 , it has received a combined signal ($x_0 \cup x_1$) from the relay node in the third time slot. It has also overheard signal x_0 transmitted by source s_0 in the first time slot. Using these two signals, d_1 can extract a copy of signal x_1 from the combined signal as follows.

Denote the combined signal received by destination node d_1 in the third time slot as

$$y_{(s_0 \cup s_1)rd_1}(t) = \alpha_r h_{rd_1} [y_{s_0 r}(t - 2T) + y_{s_1 r}(t - T)] + z_{d_1}(t), \quad \forall t \in (2T, 3T], \quad (4)$$

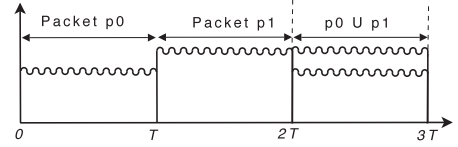


Fig. 6. Transmission behavior of ANC-CC for two sessions.

where T is the length of each time-slot in the frame, and the value of α_r is chosen as [16]

$$\alpha_r^2 = \frac{P_r}{|h_{s_0 r}|^2 P_{s_0} + |h_{s_1 r}|^2 P_{s_1} + 2\sigma_r^2}, \quad (5)$$

where P_r , P_{s_0} , and P_{s_1} are the transmission powers of nodes r , s_0 , and s_1 , respectively.

By using (1), the combined signal in (4) can be expanded as

$$y_{(s_0 \cup s_1)rd_1}(t) = \alpha_r h_{rd_1} [h_{s_0 r} x_0(t - 2T) + z_r(t - 2T) + y_{s_1 r}(t - T)] + z_{d_1}(t), \quad \forall t \in (2T, 3T]. \quad (6)$$

Using (2), (6) can be rewritten as

$$y_{(s_0 \cup s_1)rd_1}(t) = \frac{\alpha_r h_{rd_1} h_{s_0 r}}{h_{s_0 d_1}} [y_{s_0 d_1}(t - 2T) - z_{d_1}(t - 2T)] + \alpha_r h_{rd_1} y_{s_1 r}(t - T) + z_{d_1}(t) + \alpha_r h_{rd_1} z_r(t - 2T), \quad \forall t \in (2T, 3T]. \quad (7)$$

Equation (7) represents the signal that the destination node d_1 will receive in the third time slot. In the first time slot, destination node d_1 overheard the transmission of s_0 , which is given by (2) and can be rewritten as

$$y_{s_0 d_1}(t) = h_{s_0 d_1} x_0(t) + z_{d_1}(t), \quad \forall t \in [0, T]. \quad (8)$$

Since we assume that the channel gains and amplification factor are given, destination node d_1 can multiply (8), by a factor $\frac{\alpha_r h_{rd_1} h_{s_0 r}}{h_{s_0 d_1}}$, and subtract it from (7). We have

$$\begin{aligned} \hat{y}_{rd_1}(t) &= y_{(s_0 \cup s_1)rd_1}(t) - \frac{\alpha_r h_{rd_1} h_{s_0 r}}{h_{s_0 d_1}} y_{s_0 d_1}(t - 2T) \\ &= \alpha_r h_{rd_1} y_{s_1 r}(t - T) + z_{d_1}(t) + \alpha_r h_{rd_1} z_r(t - 2T) \\ &\quad - \frac{\alpha_r h_{rd_1} h_{s_0 r}}{h_{s_0 d_1}} z_{d_1}(t - 2T), \quad \forall t \in (2T, 3T]. \end{aligned} \quad (9)$$

Equation (9) represents the signal for packet p_1 that destination node d_1 can construct, using the combined signal received in the third time slot and the signal overheard in the first time slot. We find that instead of z_{d_1} , we now have a new noise term in this constructed signal, which we denote as $z_{d_1}^{\text{ANC}}$, i.e.,

$$z_{d_1}^{\text{ANC}}(t) = z_{d_1}(t) + \alpha_r h_{rd_1} z_r(t - 2T) - \frac{\alpha_r h_{rd_1} h_{s_0 r}}{h_{s_0 d_1}} z_{d_1}(t - 2T), \quad \forall t \in (2T, 3T]. \quad (10)$$

We call $z_{d_1}^{\text{ANC}}$ "ANC noise." Note that $z_{d_1}^{\text{ANC}}$ has a zero mean (because $E[z_{d_1}] = E[z_r] = 0$) and its variance is

$$\sigma_{z_{d_1}^{\text{ANC}}}^2 = \sigma_{d_1}^2 + (\alpha_r h_{rd_1})^2 \sigma_r^2 + \left(\frac{\alpha_r h_{s_0 r} h_{rd_1}}{h_{s_0 d_1}} \right)^2 \sigma_{d_1}^2, \quad (11)$$

which is larger than the original noise variance $\sigma_{d_1}^2$.

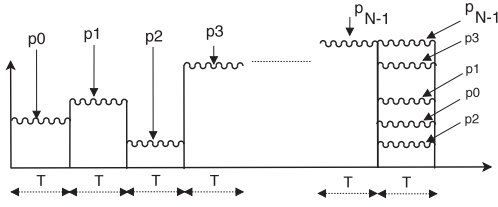


Fig. 7. Transmission behavior of ANC-CC for N sessions.

4.1.2 The N -Session Case

We now consider the general case, where there are N source-destination pairs and one relay node in the network [see Fig. 5b]. To have all N source-destination pairs share the same relay node with ANC, $(N + 1)$ time slots are needed (see Fig. 3). The signal aggregation process in this scenario follows the same token as in the two-session case. Fig. 7 shows the details in each time slot.

In this N -session case, a given destination node d_i overhears a copy of all the packets (including p_i) during the first N time slots. In order to construct the signal for the second copy of packet p_i , the destination node d_i will again follow the same procedure as in the two-session case. Now, instead of subtracting only one signal from the combined signal, the destination node will need to subtract the signals overheard from $(N - 1)$ sources. The expressions for the ANC noise can be obtained by generalizing (10) as follows:

$$\begin{aligned} z_{d_i}^{\text{ANC}}(t) &= z_{d_i}(t) + \sum_{\substack{s_j \neq s_i \\ s_j \in \mathcal{S}_r}} \alpha_r h_{rd_i} z_r(t - |\mathcal{S}_r|T) \\ &\quad - \sum_{\substack{s_j \neq s_i \\ s_j \in \mathcal{S}_r}} \frac{\alpha_r h_{rd_i} h_{s_j r}}{h_{s_j d_i}} z_{d_i}(t - |\mathcal{S}_r|T), \end{aligned} \quad (12)$$

$$\forall t \in (|\mathcal{S}_r|T, (|\mathcal{S}_r| + 1)T],$$

where \mathcal{S}_r is the set of N source nodes that are using relay r , and a general expression for the amplification factor α_r can be obtained by generalizing (5), which is

$$\alpha_r^2 = \frac{P_r}{|\mathcal{S}_r| \sigma_r^2 + \sum_{s_i \in \mathcal{S}_r} P_{s_i} |h_{s_i r}|^2}. \quad (13)$$

The variance of ANC noise can be obtained by generalizing (11), which is

$$\begin{aligned} \sigma_{z_{d_i}^{\text{ANC}}}^2 &= \sigma_{d_i}^2 + (|\mathcal{S}_r| - 1) (\alpha_r h_{rd_i})^2 \sigma_r^2 \\ &\quad + \sigma_{d_i}^2 \sum_{\substack{s_j \neq s_i \\ s_j \in \mathcal{S}_r}} \left(\frac{\alpha_r h_{s_j r} h_{rd_i}}{h_{s_j d_i}} \right)^2. \end{aligned} \quad (14)$$

We see that the variance of ANC noise at destination node d_i contains $\sigma_{d_i}^2$ and some additional new terms. These additional new terms are introduced due to the relay node employing ANC for aggregating multiple signals from sources in \mathcal{S}_r . The variance of ANC noise at the destination nodes increases with the number of sessions sharing the same relay node.

4.2 Computing Achievable Rate

4.2.1 ANC-CC

To compute the achievable rate under ANC-CC, we denote the time duration of the entire frame as t seconds. As a

result, when all N sessions are sharing the same relay node with ANC-CC (see Fig. 3), every source node and the relay node will get a time-slot of $T = \frac{t}{N+1}$ seconds. Then, the achievable rate for a session, say (s_i, d_i) , is

$$\begin{aligned} C_{\text{ANC-CC}}(s_i, r, d_i) &= \left(\frac{\frac{t}{N+1}}{t} \right) \cdot W I_{\text{ANC-CC}}(s_i, r, d_i) \\ &= \frac{W}{N+1} \cdot I_{\text{ANC-CC}}(s_i, r, d_i), \end{aligned} \quad (15)$$

where $I_{\text{ANC-CC}}(s_i, r, d_i)$ is the mutual information between s_i and d_i , and W is the available bandwidth in the network. In (15), the effective bandwidth for session (s_i, d_i) is W divided by $(N + 1)$ (N source nodes plus one relay) in the network.

To derive the mutual information $I_{\text{ANC-CC}}(s_i, r, d_i)$ between session (s_i, d_i) , we need to consider the ANC noise (14) at the destination nodes. For the signal transmitted by a source node s_i , the received signal at the relay node is

$$y_{s_i r} = h_{s_i r} x_i + z_r, \quad (16)$$

and the received signal at the corresponding destination node is

$$y_{s_i d_i} = h_{s_i d_i} x_i + z_{d_i}. \quad (17)$$

For the signal transmitted by the relay node, the desired signal at the destination node (after extraction) is

$$\hat{y}_{rd_i} = \alpha_r h_{rd_i} y_{s_i r} + z_{d_i}^{\text{ANC}},$$

which is

$$\hat{y}_{rd_i} = \alpha_r h_{rd_i} (h_{s_i r} x_i + z_r) + z_{d_i}^{\text{ANC}}, \quad (18)$$

where $z_{d_i}^{\text{ANC}}$ is given in (12) and α_r is given in (13).

We can rewrite (16), (17), and (18) into the following compact matrix form

$$\mathbf{Y} = \mathbf{H}x_i + \mathbf{B}z_r,$$

where

$$\begin{aligned} \mathbf{Y} &= \begin{bmatrix} y_{s_i d_i} \\ \hat{y}_{rd_i} \end{bmatrix}, \quad \mathbf{H} = \begin{bmatrix} h_{s_i d_i} \\ h_{rd_i} \alpha_r h_{s_i r} \end{bmatrix}, \\ \mathbf{B} &= \begin{bmatrix} 0 & 1 & 0 \\ \alpha_r h_{rd_i} & 0 & 1 \end{bmatrix}, \quad \text{and } \mathbf{Z} = \begin{bmatrix} z_r \\ z_{d_i} \\ z_{d_i}^{\text{ANC}} \end{bmatrix}. \end{aligned}$$

It was shown in [16] that we can model the above channel that combines both the direct path (s_i to d_i) and the relay path (s_i to r to d_i) as a one-input two-output complex Gaussian vector channel. The mutual information between s_i and d_i is

$$\begin{aligned} I_{\text{ANC-CC}}(s_i, r, d_i) &= \log_2 \det(\mathbf{I} + (P_{s_i} \mathbf{H} \mathbf{H}^\dagger) (\mathbf{B} E[\mathbf{Z} \mathbf{Z}^\dagger] \mathbf{B}^\dagger)^{-1}), \end{aligned} \quad (19)$$

where \mathbf{I} is the identity matrix, \dagger represents the complex conjugate transpose, $E[\cdot]$ is the expectation function, and

$$E[\mathbf{Z} \mathbf{Z}^\dagger] = \begin{bmatrix} \sigma_r^2 & 0 & 0 \\ 0 & \sigma_{d_i}^2 & 0 \\ 0 & 0 & \sigma_{z_{d_i}^{\text{ANC}}}^2 \end{bmatrix}.$$

Expanding (19) gives us the mutual information

$$I_{\text{ANC-CC}}(s_i, r, d_i) = \log_2 \left(1 + \frac{|h_{s_i d_i}|^2 P_{s_i}}{\sigma_{d_i}^2} + \frac{P_{s_i} |h_{r d_i} \alpha_r h_{s_i r}|^2}{|h_{r d_i} \alpha_r|^2 \sigma_r^2 + \sigma_{z_{d_i}}^{\text{ANC}}} \right),$$

which can be further rewritten as

$$I_{\text{ANC-CC}}(s_i, r, d_i) = \log_2 \left(1 + \text{SNR}_{s_i d_i} + \frac{\text{SNR}_{s_i r} \text{SNR}_{r d_i}}{|\mathcal{S}_r| \frac{\sigma_{d_i}^{\text{ANC}}}{\sigma_{d_i}^2} + \text{SNR}_{r d_i} + \frac{\sigma_{d_i}^{\text{ANC}}}{\sigma_{d_i}^2} \sum_{s_j \in \mathcal{S}_r} \text{SNR}_{s_j r}} \right), \quad (20)$$

where $\text{SNR}_{s_i d_i} = \frac{P_{s_i}}{\sigma_{d_i}^2} |h_{s_i d_i}|^2$, $\text{SNR}_{s_i r} = \frac{P_{s_i}}{\sigma_r^2} |h_{s_i r}|^2$, and $\text{SNR}_{r d_i} = \frac{P_r}{\sigma_{d_i}^2} |h_{r d_i}|^2$. For the special case of $|\mathcal{S}_r| = 1$, i.e., for one-session (three-node model), we have $i=0$, $\sigma_{z_{d_i}}^{\text{ANC}} = \sigma_{d_i}^2$, and (20) is reduced to

$$I_{\text{AF}}(s_i, r, d_i) = \log_2 \left(1 + \text{SNR}_{s_i d_i} + \frac{\text{SNR}_{s_i r} \text{SNR}_{r d_i}}{1 + \text{SNR}_{r d_i} + \text{SNR}_{s_i r}} \right), \quad (21)$$

which is exactly the result for the simple three-node model in [16].

For a given session, it is worth comparing its achievable rate under ANC-CC (in (15)) with the achievable rates when 1) the session performs AF CC without ANC, and 2) the session employs direct transmission. We now give the achievable rates of the latter two schemes for comparison.

4.2.2 AF CC (without ANC)

Under this scheme [16], the session performs AF CC, but the relay node does not employ ANC. Each source node and the relay node will get a time-slot of $t/2N$ (see Fig. 2). Using (21), the achievable rate for a session (s_i, d_i) is

$$C_{\text{AF}}(s_i, r, d_i) = \left(\frac{t}{2N} \right) W I_{\text{AF}}(s_i, r, d_i) = \frac{W}{2N} \log_2 \left(1 + \text{SNR}_{s_i d_i} + \frac{\text{SNR}_{s_i r} \text{SNR}_{r d_i}}{1 + \text{SNR}_{r d_i} + \text{SNR}_{s_i r}} \right). \quad (22)$$

4.2.3 Direct Transmission

Under direct transmission, a source node does not perform CC and transmits directly to its destination node. The time-slot for each source node is t/N . For a session (s_i, d_i) , the achievable rate under direct transmission is

$$C_{\text{D}}(s_i, d_i) = \left(\frac{t}{N} \right) \cdot W \log_2(1 + \text{SNR}_{s_i d_i}) = \frac{W}{N} \cdot \log_2(1 + \text{SNR}_{s_i d_i}). \quad (23)$$

5 THE CASE OF DNC-CC

We now consider the digital version of NC-CC. We organize this section as follows: in Section 5.1, we give an upper bound and a lower bound on the rates at which

source nodes can transmit data. In Section 5.2, we analyze DNC noise and the rate at which each destination node can receive. In Section 5.3, we derive the achievable rate for a session under DNC-CC.

5.1 Analyzing Transmission Rate at a Source Node

We first discuss the rate at which each source node can transmit data. We know that the relay node has to decode and then combine the signals transmitted by all the source nodes. However, the rates at which each source node can transmit varies. It is well known that in general, when multiple source nodes transmit data at different rates, the optimal DNC strategy remains unknown [3], [14], [26]. In addition to combining bits at the relay node, extraction and signal combination also need to be carried out at destination nodes. This makes designing an optimal procedure to perform DNC-CC even more complicated. So instead of trying to find an optimal DNC-CC strategy, we will present an upper bound and a lower bound for the transmission rate.

An upper bound for the transmission rate can be obtained by having every source node transmit at the maximum possible rate at which relay node can decode the data. This can be written as

$$I_{\text{DNC-CC}}^{\text{UB}}(s_i, r) = \log_2(1 + \text{SNR}_{s_i r}). \quad (24)$$

Equation (24) gives an upper bound on the transmission rate of s_i in bits/sec/Hz. This is because for any feasible (including optimal) scheme, a source node cannot transmit data at a rate that is greater than $I_{\text{DNC-CC}}^{\text{UB}}(s_i, r)$. Otherwise, the relay node will not be able to decode the signal as required in the DF scheme. As a result, the transmission rate for source s_i under any feasible scheme cannot be greater than $I_{\text{DNC-CC}}^{\text{UB}}(s_i, r)$. It is important to note that a DNC strategy to combine the data streams remains unknown when every source node transmits at its maximum possible rate. So (24) will serve as an upper bound.

Further, any feasible DNC strategy will require each source node to transmit at some transmission rate (e.g., all source nodes transmit at the same rate). This transmission rate cannot be greater than the optimal transmission rate of that source node. As a result, a feasible DNC strategy will give us a lower bound on the rate at which each source node can transmit. One feasible strategy is to denote the source node that transmits at the lowest rate as the bottleneck source node; and to limit all the source nodes to transmit at this bottleneck rate. This will enable the relay node to perform bit by bit combination of the decoded data. A lower bound on the rate at which a source node s_i can transmit can be written as

$$I_{\text{DNC-CC}}^{\text{LB}}(s_i, r) = \log_2 \left(1 + \min_{s_j \in \mathcal{S}_r} \{ \text{SNR}_{s_j r} \} \right). \quad (25)$$

5.2 Analyzing Reception Rate at a Destination Node

To study the reception rate at the destination nodes, we begin by analyzing the DNC noise. We first focus on the simple two-session network in Fig. 5a. For this network, the signal transmitted by s_0 and received by r in the first time slot is given by (1). Similarly, the signal transmitted by s_1 and received by r in the second time slot is given by (3). The

relay node r will decode the two signals, combine them using DNC, and then transmit the combined signal. The combined signal at r can be written as $(x_0 + x_1)$.

To understand the signal extraction process at a destination node, consider node d_1 . The combined signal transmitted by r and received by node d_1 can be written as

$$y_{rd_1}(t) = h_{rd_1}[x_0(t_1) + x_1(t_2)] + z_{d_1}(t), \forall t \in (2T, 3T], \quad (26)$$

where $x_0(t_1)$ is the signal transmitted by s_0 in the first time slot, and $x_1(t_2)$ is the signal transmitted by s_1 in the second time slot. Note that when all source nodes are transmitting at the same rate (i.e., the lower bound case in Section 5.1), $t_1 = t - 2T$ and $t_2 = t - T$. However, as the optimal NC strategy in general is unknown, we use general notation of t_1 and t_2 . We assume that the destination nodes know the values of t_1 and t_2 for any t (i.e., it knows the NC scheme that is employed by the relay node).

The destination node now has to subtract the x_0 signal component from (26) in order to extract x_1 . The signal for x_0 overheard by d_1 from s_0 in the first time slot is given by (2). Assuming channel gains are known, d_1 can extract the signal for x_1 by multiplying (2) by $\frac{h_{rd_1}}{h_{s_0d_1}}$ and then subtract the product from (26).¹ The extracted signal can be written as

$$\begin{aligned} \bar{y}_{rd_1}(t) &= y_{rd_1}(t) - \frac{h_{rd_1}}{h_{s_0d_1}} y_{s_0d_1}(t_1) \\ &= h_{rd_1} x_1(t_2) + z_{d_1}(t) + \frac{h_{rd_1}}{h_{s_0d_1}} z_{d_1}(t_1) \\ &\quad \forall t \in (2T, 3T]. \end{aligned} \quad (27)$$

We can see that instead of z_{d_1} , we have a new noise term, which we call ‘‘DNC noise’’ and is denoted as $z_{d_1}^{\text{DNC}}$, i.e.,

$$z_{d_1}^{\text{DNC}} = z_{d_1}(t) + \frac{h_{rd_1}}{h_{s_0d_1}} z_{d_1}(t_1), \forall t \in (2T, 3T]. \quad (28)$$

From (28), the variance of DNC noise is

$$\sigma_{z_{d_1}^{\text{DNC}}}^2 = \sigma_{d_1}^2 + \sigma_{d_1}^2 \left(\frac{h_{rd_1}}{h_{s_0d_1}} \right)^2. \quad (29)$$

For a general network with n sessions (i.e., Fig. 5b), where a group of source nodes in \mathcal{S}_r share the same relay node r , DNC noise at a destination node d_i can be obtained by generalizing (29). We have

$$\sigma_{z_{d_i}^{\text{DNC}}}^2 = \sigma_{d_i}^2 + \sigma_{d_i}^2 \sum_{s_j \in \mathcal{S}_r}^{j \neq i} \left(\frac{h_{rd_i}}{h_{s_j d_i}} \right)^2. \quad (30)$$

From (30), we can see that the variance of DNC noise increases monotonically as the number of sessions sharing the relay node.

By using the variance of DNC noise we can determine the rate at which a given destination node can receive its desired signal. Similar to the ANC-CC case, (17) and (27) can be written in a compact matrix form as

1. Another possible approach to perform signal extraction is for d_1 to first decode $y_{s_0d_1}$ and then use the extracted x_0 to perform a subtraction. However, such an approach places excessive restriction on the rate at which source nodes can transmit their signals, and is likely to perform worse than the approach we use here.

$$\mathbf{Y} = \mathbf{H}\mathbf{x}_i + \mathbf{B}\mathbf{Z}, \quad (31)$$

where

$$\mathbf{Y} = \begin{bmatrix} y_{s_i d_i} \\ \bar{y}_{rd_i} \end{bmatrix}, \quad \mathbf{H} = \begin{bmatrix} h_{s_i d_i} \\ h_{rd_i} \end{bmatrix},$$

$$\mathbf{B} = \begin{bmatrix} 1 & 0 \\ 0 & 1 \end{bmatrix}, \quad \text{and} \quad \mathbf{Z} = \begin{bmatrix} z_{d_i} \\ z_{d_i}^{\text{DNC}} \end{bmatrix}.$$

Similar to [16], we can model the above channel as a one-input two-output complex Gaussian vector channel. The rate at which destination node d_i can receive signal x_i is

$$I_{\text{DNC-CC}}(s_i \cup r, d_i) = \log_2 \det(\mathbf{I} + (\mathbf{P}\mathbf{H}\mathbf{H}^\dagger)(\mathbf{B}\mathbf{E}[\mathbf{Z}\mathbf{Z}^\dagger]\mathbf{B}^\dagger)^{-1}),$$

where

$$\mathbf{E}[\mathbf{Z}\mathbf{Z}^\dagger] = \begin{bmatrix} \sigma_{d_i}^2 & 0 \\ 0 & \sigma_{z_{d_i}^{\text{DNC}}}^2 \end{bmatrix}, \quad \text{and} \quad \mathbf{P} = \begin{bmatrix} P_{s_i} & 0 \\ 0 & P_r \end{bmatrix}.$$

Expanding the above rate equation gives us

$$I_{\text{DNC-CC}}(s_i \cup r, d_i) = \log_2 \left(1 + \frac{P_{s_i} |h_{s_i d_i}|^2}{\sigma_{d_i}^2} + \frac{P_r |h_{rd_i}|^2}{\sigma_{z_{d_i}^{\text{DNC}}}^2} \right),$$

which can be further rewritten as

$$I_{\text{DNC-CC}}(s_i \cup r, d_i) = \log_2 \left(1 + \text{SNR}_{s_i d_i} + \frac{\text{SNR}_{rd_i}}{\frac{\sigma_{z_{d_i}^{\text{DNC}}}^2}{\sigma_{d_i}^2}} \right). \quad (32)$$

From (32), we can see that the rate at which destination nodes can receive data decreases when the variance of DNC noise increases.

We now have the rate for each source node to transmit (i.e., either (24) or (25)) and the rate for each destination node to receive (i.e., (32)). For any given session, the minimum of the source transmission rate and the destination reception rate is the achievable rate for that session. As a result, the minimum of (24) and (32) gives us an upper bound for the mutual information for session (s_i, d_i) . Similarly, the minimum of (25) and (32) gives us a lower bound for the mutual information for a session (s_i, d_i) under DNC-CC.

5.3 Computing Achievable Rate

Similar to the analog case, we assume that each frame has a length of t (seconds) and each time slot in the frame has a length of T . Then, $T = \frac{t}{N+1}$. Under such setting, we can write the upper bound on the achievable rate of (s_i, d_i) for DNC-CC as

$$\begin{aligned} C_{\text{DNC-CC}}^{\text{UB}}(s_i, r, d_i) \\ = \frac{W}{N+1} \cdot \min\{I_{\text{DNC-CC}}^{\text{UB}}(s_i, r), I_{\text{DNC-CC}}(s_i \cup r, d_i)\}, \end{aligned} \quad (33)$$

and the lower bound on the achievable rate of (s_i, d_i) as

$$\begin{aligned} C_{\text{DNC-CC}}^{\text{LB}}(s_i, r, d_i) \\ = \frac{W}{N+1} \cdot \min\{I_{\text{DNC-CC}}^{\text{LB}}(s_i, r), I_{\text{DNC-CC}}(s_i \cup r, d_i)\}. \end{aligned} \quad (34)$$

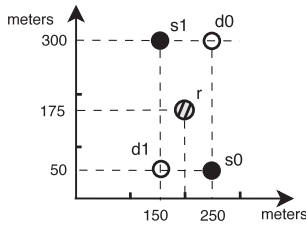


Fig. 8. A network topology where NC is a friend of CC.

TABLE 2
Comparison of Achievable Rates When ANC Is a Friend

Session	ANC-CC (Mb/s)	AF CC (Mb/s)	Direct Transmission (Mb/s)
(s_0, d_0)	23.75	22.09	19.22
(s_1, d_1)	23.75	22.09	19.22

Note that when $|\mathcal{S}_r| = 1$, i.e., one-session (three-node model), we have $\sigma_{z_{\text{DNC}}}^2 = \sigma_{d_i}^2$, and both (33) (upper bound) and (34) (lower bound) reduce to

$$C_{DF}(s_i, r, d_i) = \frac{W}{2} \min \left\{ \log_2(1 + \text{SNR}_{s_i r}), \log_2(1 + \text{SNR}_{s_i d_i} + \text{SNR}_{r d_i}) \right\},$$

which is exactly the result for the three-node model given in [16].

DF CC (without DNC). It is worth comparing the achievable rate under DNC-CC with DF CC when DNC is not used. Under the latter scheme, every source node and the relay node gets equal time slot duration of $\frac{t}{2N}$. The achievable rate of a session (s_i, d_i) is [16]

$$C_{DF}(s_i, r, d_i) = \frac{W}{2N} \min \left\{ \log_2 \left(1 + \frac{|h_{s_i r}|^2 P_{s_i}}{\sigma_r^2} \right), \log_2 \left(1 + \frac{|h_{r d_i}|^2 P_r}{\sigma_{d_i}^2} + \frac{|h_{s_i d_i}|^2 P_{s_i}}{\sigma_{d_i}^2} \right) \right\}. \quad (35)$$

6 NUMERICAL RESULTS

In this section, we present some numerical results to show the impact of NC on CC, in the light of NC noise. We assume that the total bandwidth in the network $W = 22$ MHz [10]. All source nodes transmit with 1 W of power. The variance of Gaussian noise at each node is 10^{-10} W, and the path loss index is 4. For simplicity, the channel gain $|h_{uv}|^2$ between two nodes is modeled as d_{uv}^{-4} , where d_{uv} is the distance between u and v , and 4 is the path loss index.

The results are divided into two parts. In the first part, we use simple two-session networks to illustrate that NC can be either a friend or a foe of CC, depending on network settings. So a blind use of NC in CC is not advisable. The second part consists of a general network with multiple sessions. Here, we quantify the impact of DNC noise and ANC noise on the achievable rate of individual sessions. Our results show that as the number of sessions that share the same relay node increases, the benefit of NC in CC diminishes, gradually switching NC from a friend to a foe.

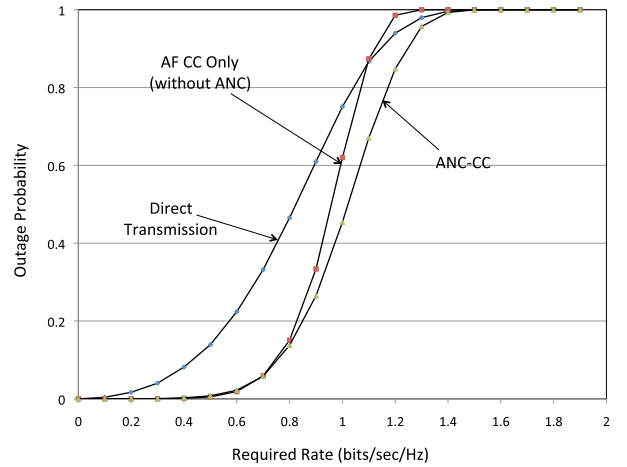
Fig. 9. Outage probabilities of session $s_0 \rightarrow d_0$ when ANC is a friend.

TABLE 3
Comparison of Achievable Rates When DNC Is a Friend

Session	DNC-CC (Mb/s)		DF CC (Mb/s)	Direct Transmission (Mb/s)
	LB	UB		
(s_0, d_0)	33.22	33.22	26.09	19.22
(s_1, d_1)	33.22	33.22	26.09	19.22

6.1 Two-Session Networks

6.1.1 NC as a Friend

We first show that in certain network settings, NC-CC can offer better data transmission rates than CC or direct transmission schemes. A network topology illustrating this case is shown in Fig. 8.

The analog case (ANC-CC). For ANC-CC, the results are shown in Table 2 and Fig. 9. There are four columns in Table 2. The first column shows the source and destination nodes of each session. The second column shows the achievable rates under ANC-CC (i.e., based on (15)). The third column shows the achievable rate for each session when the session performs AF CC without the use of ANC (i.e., based on (22)). The last column shows the achievable rate of the sessions under direct transmission (i.e., based on (23)).

We can see that for the topology in Fig. 8, the achievable rates under ANC-CC are higher than the achievable rates under AF CC without ANC, as well as the rates under direct transmission. Fig. 9 shows the results for the outage probability of session $s_0 \rightarrow d_0$ under ANC-CC, AF CC, and direct transmission schemes. The results for session $s_1 \rightarrow d_1$ are similar and are thus omitted. For each scheme, the outage probability is computed by counting the number of outages under 10,000 channel realizations. We assume that all channels in the network are Rayleigh faded. Fig. 9 shows that the outage probability of session $s_0 \rightarrow d_0$ under ANC-CC is lower than that under AF CC scheme and direct transmission.

The digital case (DNC-CC). For DNC-CC, the results are shown in Table 3 and Fig. 10. The columns in Table 3 are similar to those in Table 2, except that the achievable rate under DNC-CC is represented by an upper bound and a lower bound in the second and third columns. By noting that the upper and lower bounds for both sessions are identical, we conclude that the rates in columns 2 and 3 are

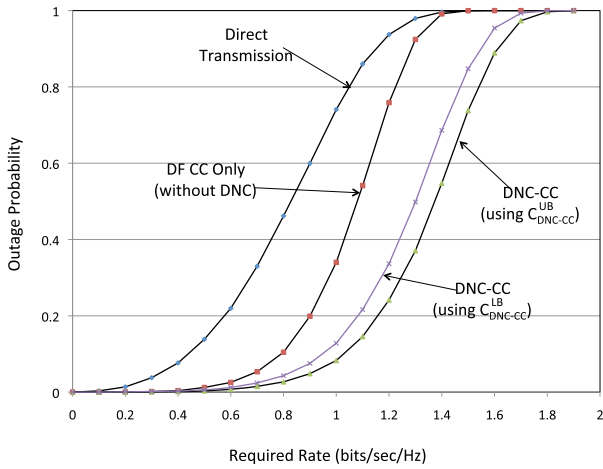


Fig. 10. Outage probabilities of session (s_0, d_0) when DNC is a friend.

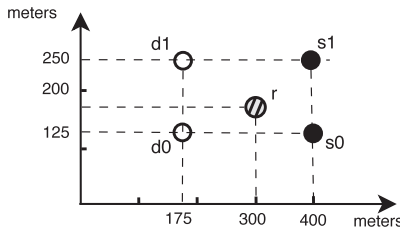


Fig. 11. A network topology where NC is a foe of CC.

TABLE 4
Comparison of Achievable Rates When ANC Is a Foe

Session	ANC-CC (Mb/s)	AF CC (Mb/s)	Direct Transmission (Mb/s)
(s_0, d_0)	20.50	24.45	24.06
(s_1, d_1)	18.20	22.30	24.06

the optimal rates. We can see that the achievable rates under DNC-CC (columns 2 and 3) are better than those under DF CC without DNC (column 4) as well as the rate under direct transmission (i.e., the last column in Table 3). Further, Fig. 10 shows that the outage probabilities of session $s_0 \rightarrow d_0$ under DNC-CC are also lower than those under DF CC and direct transmission.

Note that the above results for ANC-CC and DNC-CC can also be explained intuitively. To extract the desired signal from the combined signal, node d_0 has to subtract the overheard signal from s_1 . From Fig. 8, we see that since s_1 is closer to d_0 , this gives d_0 a better reception of the signal from s_1 . As a result, the NC noise component in the extracted signal at d_0 is small, which makes NC a friend of CC. Similar discussion also holds for session (s_1, d_1) in Fig. 8.

6.1.2 NC as a Foe

We now show that NC may not always benefit CC. A network topology illustrating this case is shown in Fig. 11.

The analog case (ANC-CC). For ANC-CC, the results are shown in Table 4 and Fig. 12. Table 4 shows that for both sessions, the achievable rates under ANC-CC (column 2) are lower than those under AF CC and direct transmission, respectively. Fig. 12 shows that over a wide range, the outage probabilities of session $s_0 \rightarrow d_0$ under ANC-CC are higher than those under AF CC and direct transmission.

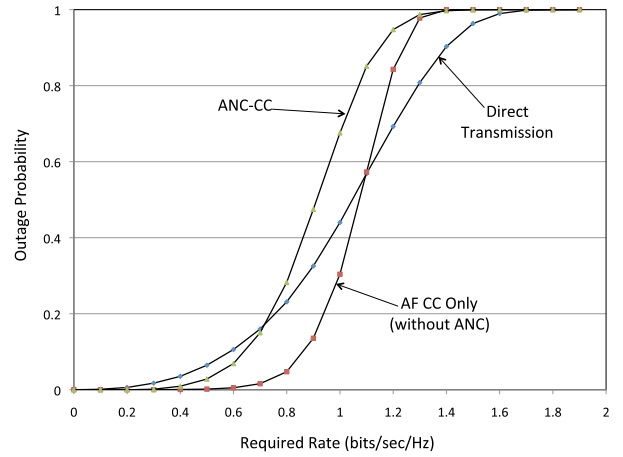


Fig. 12. Outage probabilities of session $s_0 \rightarrow d_0$ when ANC is a foe.

TABLE 5
Comparison of Achievable Rate When DNC Is a Foe

Session	DNC-CC (Mb/s)		DF CC (Mb/s)	Direct Transmission (Mb/s)
	LB	UB		
(s_0, d_0)	19.66	19.66	26.98	24.06
(s_1, d_1)	19.59	19.59	24.95	24.06

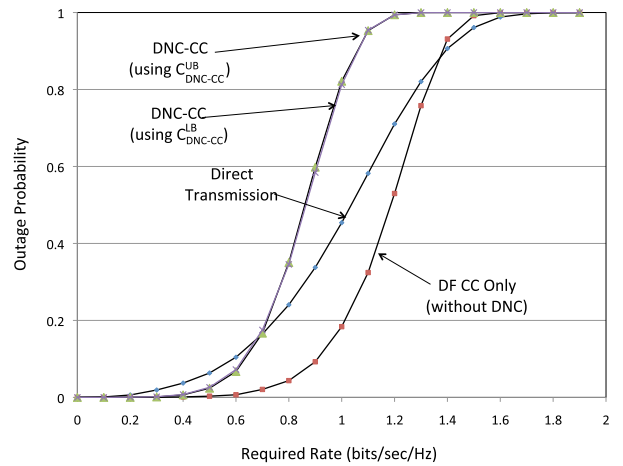


Fig. 13. Outage probabilities of session $s_0 \rightarrow d_0$ when DNC is a foe.

The digital case (DNC-CC). Similar to the analog case, Table 5 shows that for both sessions, the achievable rates under DNC-CC (columns 2 and 3) are lower than those under DF CC and direct transmission, respectively. Fig. 13 shows that over a wide range, the outage probabilities of session $s_0 \rightarrow d_0$ under DNC-CC are higher than those under DF CC and direct transmission. Note that in Fig. 13, the plots for the lower and upper bounds on the outage probability under the DNC-CC scheme overlap with each other.

Note that the above results for ANC-CC and DNC-CC can also be explained intuitively. To extract the desired signal from the combined signal, node d_0 has to subtract the signal overheard from s_1 . From Fig. 11, we see that source s_1 is far away from d_0 . This results in weaker reception of s_1 's signal at d_0 . Therefore, the NC noise component in the extracted signal at d_0 is high, which makes NC a foe of CC. Similar discussion also holds for session (s_1, d_1) in Fig. 11. However, we can see that the effect of NC noise on (s_1, d_1) is more than that on (s_0, d_0) . This can be explained by

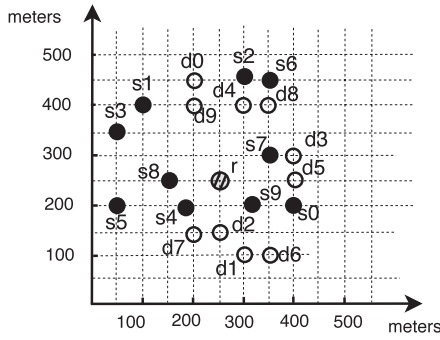


Fig. 14. A 10-session one-relay network topology.

observing that node d_1 is farther away from r as compared to node d_0 , resulting in comparatively weaker reception of network coded signal at d_1 .

6.1.3 Summary

The above two scenarios illustrate that NC can be either a friend or a foe of CC. That is, the NC noise infused at the destination nodes could undermine the time slot advantage of NC-CC. When NC noise is sufficiently large, the advantage of NC-CC diminishes and NC becomes a foe of CC.

6.2 A General Multisession Network

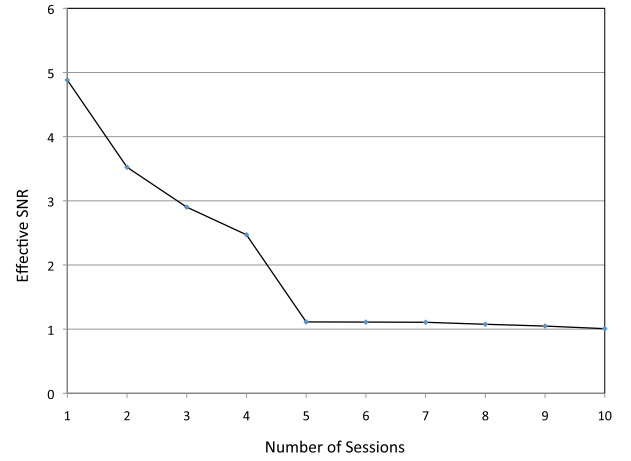
In this section, we consider a general network with multiple sessions. The network topology is shown in Fig. 14, where we have 10 sessions and one relay node. We show that when more sessions employ NC-CC and share the same relay node, NC noise at destination nodes will increase. This increase in NC noise will have a direct impact on the effective SNR and the achievable rate of individual sessions. As a result, when the amount of NC noise increases beyond a certain threshold, NC will switch from a friend to a foe of CC. We chose session $s_0 \rightarrow d_0$ in our study to demonstrate these findings under both ANC-CC and DNC-CC.

The analog case (ANC-CC). To start with, all the sessions are active, but only one session ($s_0 \rightarrow d_0$) is using the relay node r to perform AF CC. The effective bandwidth for each session is $W/10$. We first determine the effect of adding more sessions on the effective SNR of $s_0 \rightarrow d_0$. Here, the effective SNR for a session $s_i \rightarrow d_i$ is defined based on (15), i.e.,

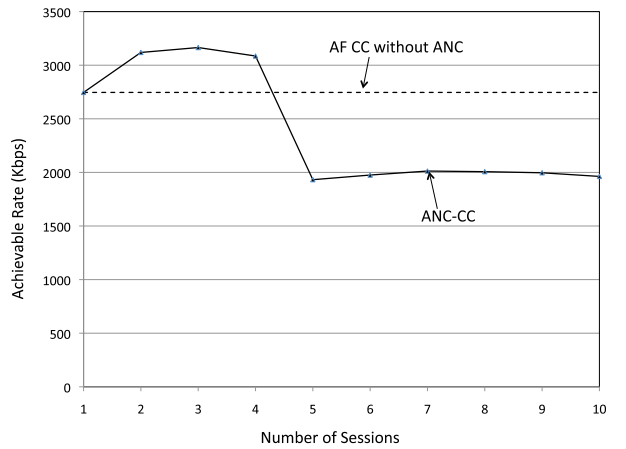
$$\text{SNR}_{\text{eff}}^{\text{ANC}}(s_i, r, d_i) = \text{SNR}_{s_i d_i} + \frac{\text{SNR}_{s_i r} \text{SNR}_{r d_i}}{|\mathcal{S}_r| \frac{\sigma_{d_i}^2}{\sigma_r^2} + \text{SNR}_{r d_i} + \frac{\sigma_{d_i}^2}{\sigma_r^2} \sum_{s_j \in \mathcal{S}_r} \text{SNR}_{s_j r}}, \quad (36)$$

where \mathcal{S}_r is the set for those source nodes using relay node r .

Since only one session (i.e., ($s_0 \rightarrow d_0$)) is using the relay node initially, the value of $N(= |\mathcal{S}_r|)$ in (36) will be one for session $s_0 \rightarrow d_0$, and \mathcal{S}_r will contain only s_0 . Then, we let session $s_1 \rightarrow d_1$ also share the relay node. Now both $s_0 \rightarrow d_0$ and $s_1 \rightarrow d_1$ are employing ANC-CC, and the other eight sessions are using direct transmission. Note that now, the value of $N(= |\mathcal{S}_r|)$ in (36) for these two sessions will be two,



(a) Impact on effective SNR for session $s_0 \rightarrow d_0$.



(b) Impact on achievable rate for session $s_0 \rightarrow d_0$.

Fig. 15. The impact on session $s_0 \rightarrow d_0$ as more sessions share the same relay node.

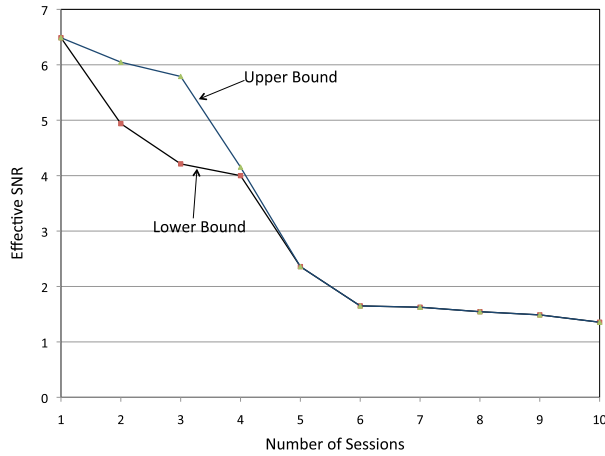
and \mathcal{S}_r will contain $\{s_0, s_1\}$. The process continues until all 10 sessions share the same relay node.

We plot the effective SNR of session $s_0 \rightarrow d_0$ as more sessions are using the same relay in Fig. 15a. We can see that as more sessions start using the relay node, the effective SNR of session $s_0 \rightarrow d_0$ decreases. This is due to the increase in the ANC noise at the destination node for session $s_0 \rightarrow d_0$.

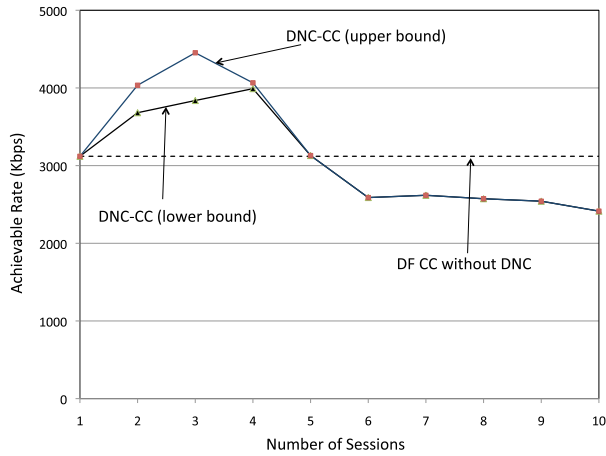
This reduction in the effective SNR of session $s_0 \rightarrow d_0$ affects the achievable rate of this session. This impact is illustrated in Fig. 15b. We plot two curves in Fig. 15b. The solid curve shows the achievable rate of session $s_0 \rightarrow d_0$, which is calculated using (15). The straight dotted line shows the achievable rate of session $s_0 \rightarrow d_0$ when ANC is not used (i.e., (22)). In Fig. 15b, we find that NC remains a friend of CC for session $s_0 \rightarrow d_0$ initially due to the time-slot benefit of NC. However, as more sessions start sharing the same relay node, the adverse effect of ANC noise at d_0 starts to increase, and the achievable rate of session $s_0 \rightarrow d_0$ starts to decrease. Finally, when five sessions share the relay node, the ANC noise reaches a point where the time-slot benefit of ANC-CC is no longer able to offset the adverse effect of ANC noise. At this point, NC switches from a friend to a foe of CC.

TABLE 6
Comparison of Various Data Communication Schemes with ANC-CC for a 10-Session Network

Session	ANC-CC (Mb/s)	AF CC (Mb/s)	Direct Transmission (Mb/s)
(s_0, d_0)	1.92	2.68	2.02
(s_1, d_1)	1.36	2.49	1.41
(s_2, d_2)	2.00	2.70	2.05
(s_3, d_3)	1.40	2.34	1.50
(s_4, d_4)	4.81	4.43	4.37
(s_5, d_5)	0.92	2.13	0.97
(s_6, d_6)	1.44	2.20	1.55
(s_7, d_7)	5.53	5.49	5.39
(s_8, d_8)	3.89	3.78	3.84
(s_9, d_9)	4.86	4.43	4.37



(a) Impact on effective SNR for session $s_0 \rightarrow d_0$.



(b) Impact on achievable rate for session $s_0 \rightarrow d_0$.

Fig. 16. The impact on session $s_0 \rightarrow d_0$ as more sessions share the same relay node.

We now consider the final instance when all the sessions in the network are using the same relay node to perform ANC-CC. Table 6 shows the achievable rates of all the sessions in the network under different transmission schemes (similar to Tables 2 and 4). As one can see, there is no definitive statement on which scheme is better, when considering all 10 sessions jointly.

The digital case (DNC-CC). Following the same process as in the analog case, we let multiple sessions share the same relay node. Initially, only one session ($s_0 \rightarrow d_0$) is using the

TABLE 7
Comparison of Various Data Communication Schemes with DNC-CC for a 10-Session Network

Session	DNC-CC (Mb/s)		DF CC (Mb/s)	Direct Transmission (Mb/s)
	LB	UB		
(s_0, d_0)	2.36	2.36	3.05	2.02
(s_1, d_1)	1.55	1.55	2.70	1.41
(s_2, d_2)	2.32	2.32	2.50	2.05
(s_3, d_3)	1.77	1.77	2.44	1.50
(s_4, d_4)	4.24	4.24	4.55	4.37
(s_5, d_5)	1.14	1.14	2.84	0.97
(s_6, d_6)	1.60	1.60	2.44	1.55
(s_7, d_7)	4.43	5.02	6.32	5.39
(s_8, d_8)	3.69	3.69	3.89	3.84
(s_9, d_9)	4.35	4.35	4.55	4.37

relay node r to perform DF CC. Afterward, other sessions start sharing the relay node one by one. The process continues until all 10 sessions share the same relay node.

Similar to the analog case, Fig. 16b shows that the reduction in effective SNR directly impacts the achievable rate of $s_0 \rightarrow d_0$ in DNC-CC. We can see that the achievable rate for session $s_0 \rightarrow d_0$ under DNC-CC falls below the achievable rate under DF CC when five or more sessions share the relay node. This is the point where NC switches from a friend to a foe.

Table 7 shows the achievable rates when all 10 sessions in the network share the same relay node under DNC-CC (similar to Table 6 for the analog case). We observe that the achievable rate under DNC-CC is lower than that under the DF CC scheme for all the sessions. This shows that by having all the sessions share the same relay node, the benefit of NC in CC diminishes.

Fig. 16a shows the effect of adding more sessions on the effective SNR of session $s_0 \rightarrow d_0$. The lower and the upper bounds on the effective SNR under DNC-CC are defined based on (33) and (34), and are written as

$$\text{SNR}_{\text{eff-DNC}}^{\text{LB}}(s_i, r, d_i) = \min \left\{ \min_{s_j \in \mathcal{S}_r} \{ \text{SNR}_{s_j r} \}, \left(\text{SNR}_{s_i d_i} + \frac{\text{SNR}_{r d_i}}{\frac{\sigma_{\text{DNC}}^2}{\sigma_{d_i}^2}} \right) \right\},$$

$$\text{SNR}_{\text{eff-DNC}}^{\text{UB}}(s_i, r, d_i) = \min \left\{ \text{SNR}_{s_j r}, \left(\text{SNR}_{s_i d_i} + \frac{\text{SNR}_{r d_i}}{\frac{\sigma_{\text{DNC}}^2}{\sigma_{d_i}^2}} \right) \right\}.$$

We can see that after four sessions, the plot for the lower bound and upper bound coincides with each other.

Summary. From the above results, we find that NC can benefit CC only when the number of sessions sharing the same relay node is small. As such number increases, NC noise also increases (both in the analog case and the digital case), and the benefit of NC in CC diminishes. Note that the quantitative effect of ANC on AF-CC is different from that of DNC on DF-CC. This is due to the physical difference between the two schemes. A quantitative comparison between the two schemes is beyond the scope of this paper.

7 CONCLUSION

In this paper, we investigated the fundamental problem of how NC can affect the performance of CC. In contrary to current perception, NC can be both a friend or a foe of CC, depending on the underlying network setting. The reason for such uncertainty is the existence of NC noise, which is the key factor that hinders the performance of NC-CC. In this paper, we formalized the concept of NC noise and characterized it mathematically both for the analog case (ANC-CC) and digital case (DNC-CC). We also derived mutual information and achievable rate calculations under ANC-CC and DNC-CC. Using numerical results, we demonstrated the impact of NC on CC. Our results offer new understanding on NC-CC and provide guidelines on its future application in practice.

Our findings in this paper lay the foundation for the design of MAC and network layer protocols for NC-CC. Here, we briefly discuss some important problems that we envision for MAC/network layer protocol design. We start with the simple problem where there are multiple sessions and only one relay node. For a given objective, a MAC problem could be how to group sessions and assign time slot for each session. Note that the problem is further complicated by the fact that some sessions may be better-off by using direct transmission instead of NC-CC. In the case when multiple relay nodes are present, the problem becomes much harder. At the network layer, when data transport between a source and its destination node requires multiple hops, we need to consider how to assign an available node for physical layer relay (NC-CC) or network layer relay (i.e., the multihop relay). The solutions to these problems remain open and should be explored as future work.

ACKNOWLEDGMENTS

The work of Y.T. Hou, S.F. Midkiff, S. Sharma, and Y. Shi was supported in part by the US National Science Foundation under Grant CNS-1064953. The work of S. Kompella was supported in part by the ONR. This work was completed while S. Sharma and J. Liu were with Virginia Tech, Blacksburg, Virginia.

REFERENCES

- [1] R. Ahlswede, N. Cai, S-Y.R. Li, and R.W. Yeung, "Network Information Flow," *IEEE Trans. Information Theory*, vol. 46, no. 4, pp. 1204-1216, July 2000.
- [2] X. Bao and J. Li, "Adaptive Network Coded Cooperation (ANCC) for Wireless Relay Networks: Matching Code-on-Graph with Network-on-Graph," *IEEE Trans. Wireless Comm.*, vol. 7, no. 2, pp. 574-583, Feb. 2008.
- [3] M. Chen, M. Ponec, S. Sengupta, J. Li, and P.A. Chou, "Utility Maximization in Peer-to-Peer Systems," *Proc. ACM SIGMETRICS Int'l Conf. Measurement and Modeling of Computer Systems*, pp. 169-180, June 2008.
- [4] T.M. Cover and A. El Gamal, "Capacity Theorems for the Relay Channel," *IEEE Trans. Information Theory*, vol. 25, no. 5, pp. 572-584, Sept. 1979.
- [5] M.O. Damen and A.R. Hammons, "Delay-Tolerant Distributed-TAST Codes for Cooperative Diversity," *IEEE Trans. Information Theory*, vol. 53, no. 10, pp. 3755-3773, Oct. 2007.
- [6] D. Gunduz and E. Erkip, "Opportunistic Cooperation by Dynamic Resource Allocation," *IEEE Trans. Wireless Comm.*, vol. 6, no. 4, pp. 1446-1454, Apr. 2007.
- [7] O. Gurewitz, A. de Baynast, and E.W. Knightly, "Cooperative Strategies and Achievable Rate for Tree Networks with Optimal Spatial Reuse," *IEEE Trans. Information Theory*, vol. 53, no. 10, pp. 3596-3614, Oct. 2007.
- [8] The Network Coding Home Page, <http://www.ifp.uiuc.edu/~koetter/NWC/index.html>, 2012.
- [9] T.E. Hunter and A. Nosratinia, "Diversity through Coded Cooperation," *IEEE Trans. Wireless Comm.*, vol. 5, no. 2, pp. 283-289, Feb. 2006.
- [10] *IEEE 802.11: Wireless LAN Medium Access Control (MAC) and Physical Layer (PHY) Specifications*, <http://standards.ieee.org/getieee802/download/802.11-2007.pdf>, 2012.
- [11] S. Katti, H. Rahul, W. Hu, D. Katabi, M. Medard, and J. Crowcroft, "XORs in the Air: Practical Wireless Network Coding," *Proc. ACM SIGCOMM*, pp. 497-510, Sept. 2006.
- [12] S. Katti, S. Gollakotta, and D. Katabi, "Embracing Wireless Interference: Analog Network Coding," *Proc. ACM SIGCOMM*, pp. 397-408, Aug. 2007.
- [13] A.E. Khandani, J. Abounadi, E. Modiano, and L. Zheng, "Cooperative Routing in Static Wireless Networks," *IEEE Trans. Comm.*, vol. 55, no. 11, pp. 2185-2192, Nov. 2007.
- [14] M. Kim, M. Medard, U-M. O'Reilly, and D. Traskov, "An Evolutionary Approach to Inter-Session Network Coding," *Proc. IEEE INFOCOM*, pp. 450-458, Apr. 2009.
- [15] G. Kramer, I. Maric, and R.D. Yates, "Foundations and Trends in Networking," *Cooperative Communications*, Now Publishers, June 2007.
- [16] J.N. Laneman, D.N.C. Tse, and G.W. Wornell, "Cooperative Diversity in Wireless Networks: Efficient Protocols and Outage Behavior," *IEEE Trans. Information Theory*, vol. 50, no. 12, pp. 3062-3080, Dec. 2004.
- [17] C. Peng, Q. Zhang, M. Zhao, and Y. Yao, "On the Performance Analysis of Network-Coded Cooperation in Wireless Networks," *Proc. IEEE INFOCOM*, pp. 1460-1468, May 2007.
- [18] S. Savazzi and U. Spagnolini, "Energy Aware Power Allocation Strategies for Multihop-Cooperative Transmission Schemes," *IEEE J. Selected Areas in Comm.*, vol. 25, no. 2, pp. 318-327, Feb. 2007.
- [19] Y.E. Sagduyu, D. Guo, and R. Berry, "On the Delay and Throughput of Digital and Analog Network Coding for Wireless Broadcast," *Proc. 44th Ann. Conf. Information Sciences and Systems*, pp. 534-539, Mar. 2008.
- [20] A. Scaglione, D.L. Goeckel, and J.N. Laneman, "Cooperative Communications in Mobile Ad Hoc Networks," *IEEE Signal Processing Magazine*, vol. 23, no. 5, pp. 18-29, Sept. 2006.
- [21] A. Sendonaris, E. Erkip, and B. Aazhang, "User Cooperation Diversity—Part I: System Description," *IEEE Trans. Comm.*, vol. 51, no. 11, pp. 1927-1938, Nov. 2003.
- [22] A. Sendonaris, E. Erkip, and B. Aazhang, "User Cooperation Diversity—Part II: Implementation Aspects and Performance Analysis," *IEEE Trans. Comm.*, vol. 51, no. 11, pp. 1939-1948, Nov. 2003.
- [23] E.C. van der Meulen, "Three Terminal Communication Channels," *Advances in Applied Probability*, vol. 3, pp. 120-154, 1971.
- [24] L. Xiao, T.E. Fuja, J. Kliewer, and D.J. Costello, "A Network Coding Approach to Cooperative Diversity," *IEEE Trans. Information Theory*, vol. 53, no. 10, pp. 3714-3722, Oct. 2007.
- [25] H. Xu and B. Li, "XOR-Assisted Cooperative Diversity in OFDMA Wireless Networks: Optimization Framework and Approximation Algorithms," *Proc. IEEE INFOCOM*, pp. 2141-2149, Apr. 2009.
- [26] X. Yan, R.Y. Yeung, and Z. Zhang, "The Capacity Region for Multi-Source Multi-Sink Network Coding," *Proc. IEEE Symp. Information Theory*, pp. 116-120, June 2007.
- [27] E.M. Yeh and R.A. Berry, "Throughput Optimal Control of Cooperative Relay Networks," *IEEE Trans. Information Theory*, vol. 53, no. 10, pp. 3827-3833, Oct. 2007.



Sushant Sharma received the BE degree in computer engineering from the University of Pune, India, in 2002, the MS degree in computer science from the University of New Mexico, Albuquerque, in 2005, and the PhD degree in computer science from the Virginia Polytechnic Institute and State University, Blacksburg, in 2010. Currently, he is working as a research associate in the Computational Science Center at Brookhaven National Laboratory, Upton, New

York. His research interests include developing novel algorithms to solve optimization problems in wired and wireless networks.



Yi Shi received the BS degree from the University of Science and Technology of China, Hefei, in 1998, the MS degree from the Institute of Software, Chinese Academy of Science, Beijing, in 2001, a second MS degree from the Virginia Polytechnic Institute and State University (Virginia Tech), Blacksburg, in 2003, all in computer science, and the PhD degree in computer engineering from Virginia Tech in 2007. Currently, he is working as a research

scientist in the Department of Electrical and Computer Engineering at Virginia Tech. His research focuses on algorithms and optimization for cognitive radio networks, MIMO and cooperative communication networks, sensor networks, and ad hoc networks. He was a recipient of the IEEE INFOCOM 2008 Best Paper Award, the only Best Paper Award runner-up at IEEE INFOCOM 2011, and the Chinese Government Award for Outstanding PhD Students Abroad in 2006. He has served as a TPC member for many major international conferences (including ACM MobiHoc 2009 and IEEE INFOCOM 2009-2012).



Jia Liu received the dual BS degrees in electrical engineering and computer science, and the MS degree in electrical engineering from the South China University of Technology in 1996 and 1999, respectively, and the PhD degree in electrical and computer engineering from the Virginia Polytechnic Institute and State University in February 2010. Since April 2010, he has worked as a postdoctoral researcher in the Department of Electrical and Computer

Engineering at Ohio State University. His research interests include the areas of optimization of communication systems and networks, theoretical foundations of cross-layer optimization on wireless networks, algorithms design, and information theory. He was a corecipient of the Bell Labs President Gold Award in 2001, the IEEE ICC 2008 Wireless Networking Symposium Best Paper Award, and the Chinese Government Award for Outstanding PhD Student Abroad in 2008. From 1999-2003, he was a member of the technical staff at Bell Labs, Lucent Technologies, Beijing, China. He is a member of Tau Beta Pi and HKN.



Y. Thomas Hou received the PhD degree in electrical engineering from the Polytechnic Institute of New York University in 1998. From 1997 to 2002, he was a researcher at Fujitsu Laboratories of America, Sunnyvale, California. Since 2002, he has been with the Virginia Polytechnic Institute and State University, the Bradley Department of Electrical and Computer Engineering, Blacksburg, where he is now an associate professor. Currently, he is serving as

an area editor of the *IEEE Transactions on Wireless Communications*, an editor for the *IEEE Transactions on Mobile Computing*, *IEEE Wireless Communications*, *ACM/Springer Wireless Networks (WINET)*, and *Elsevier Ad Hoc Networks*. He was a past associate editor of the *IEEE Transactions on Vehicular Technology*. He was technical program cochair of IEEE INFOCOM 2009. Recently, he coedited a textbook titled *Cognitive Radio Communications and Networks: Principles and Practices* (Academic Press/Elsevier, 2010). His research interests include cross-layer design and optimization for cognitive radio wireless networks, cooperative communications, MIMO-based ad hoc networks, and new interference management schemes for wireless networks. He was a recipient of an Office of Naval Research (ONR) Young Investigator Award (2003) and a US National Science Foundation CAREER Award (2004) for his research on optimizations and algorithm design for wireless ad hoc and sensor networks.



Sastry Kompella received the PhD degree in electrical and computer engineering from the Virginia Polytechnic Institute and State University, Blacksburg, in 2006. Currently, he is working as a researcher in the Information Technology Division, US Naval Research Laboratory, Washington, DC. His research focuses on complex problems in cross-layer optimization and scheduling in wireless networks.



Scott F. Midkiff received the BSE and PhD degrees from Duke University, Durham, North Carolina, and the MS degree from Stanford University, California, all in electrical engineering. Currently, he is working as a professor and department head in the Bradley Department of Electrical and Computer Engineering, Virginia Polytechnic Institute and State University (Virginia Tech), Blacksburg. He worked at Bell Laboratories and held a visiting position at

Carnegie Mellon University, Pittsburgh, Pennsylvania. He joined Virginia Tech in 1986. During 2006-2009, he served as a program director at the US National Science Foundation. His research and teaching interests include wireless and ad hoc networks, network services for pervasive computing, and cyber-physical systems.

► For more information on this or any other computing topic, please visit our Digital Library at www.computer.org/publications/dlib.